

QCD thermodynamics at zero and non-zero density

Christian Schmidt (for RBC-Bielefeld and HotQCD Collaborations)

Universität Bielefeld, Fakultät für Physik, D-33615 Bielefeld, Germany.

Abstract

We present results on the QCD equation of state, obtained with two different improved dynamical staggered fermion actions and almost physical quark masses. Lattice cut-off effects are discussed in detail as results for three different lattice spacings are available now, i.e. results have been obtained on lattices with temporal extent of $N_\tau = 4, 6$ and 8 . Furthermore we discuss the Taylor expansion approach to non-zero baryon chemical potential by means of an expansion of the pressure. We use the expansion coefficients to calculate various fluctuations and correlations among hadronic charges. We find that the correlations reproduce the qualitative behavior of the resonance gas model below T_c and start to agree with the free gas predictions for $T \gtrsim 1.5T_c$.

Key words: Lattice gauge theory, Finite-temperature field theory, Lattice QCD calculations, Quark-gluon plasma

PACS: 11.15.Ha, 11.10.Wx, 12.38.Gc, 12.38.Mh

1. Introduction

A detailed and comprehensive understanding of the thermodynamics of quarks and gluons, e.g. of the equation of state is most desirable and of particular importance for the phenomenology of relativistic heavy ion collisions. Lattice regularized QCD simulations at non-zero temperatures have been shown to be a very successful tool in analyzing the non-perturbative features of the quark-gluon plasma. Driven by both, the exponential growth of the computational power of recent super-computers as well as by drastic algorithmic improvements one is now able to simulate dynamical quarks and gluons on fine lattices with almost physical masses.

2. Lattice parameter and scale setting

We perform calculations on lattices of extent $16^3 \times 4$, $24^3 \times 6$, using the p4fat3 action [1] and $32^3 \times 8$ with both p4fat3 and asqtad actions. The latter calculations are

still preliminary and are currently performed by the HotQCD collaboration [2]. For the generation of gauge configurations we use the exact RHMC algorithm [3]. For each finite temperature calculation we perform a corresponding zero temperature calculation on a lattice of at least the size N_σ^4 , where N_σ is the spatial extent of the finite temperature lattices.

The simulations are done on a line of constant physics (LCP), i.e. the quark masses are kept constant in physical units. In practice, this has been obtained by tuning the bare quark masses such that the meson masses of e.g. pion, kaon and pseudo-scalar strange meson $\bar{s}s$ stay constant in the QCD vacuum as we change the value of the coupling. The strange quark mass was always fixed to its physical value, by fixing kaon and $\bar{s}s$ to their corresponding physical values [1]. We find that the LCP can, to a good approximation, be parameterized by a constant ratio of the bare quark masses. Most calculations are done on a LCP which corresponds to a pion mass of about 220 MeV. We do, however, also show preliminary results with a light quark mass corresponding to about 150 MeV for the lightest pseudo-scalar mass [4].

To set the temperature scale in physical units, we determine two distance scales, r_0 and r_1 , from the zero temperature static quark potential

$$\left(r^2 \frac{dV_{\bar{q}q}(r)}{dr} \right)_{r=r_0} = 1.65, \quad \left(r^2 \frac{dV_{\bar{q}q}(r)}{dr} \right)_{r=r_1} = 1.0 \quad (1)$$

The ratio of both scales is only slightly quark mass dependent. It has been determined in both discretization schemes consistently, $r_0/r_1 = 1.4636(60)$ (p4fat3 [1]) and $1.474(7)(18)$ (asqtad [5]). The distance scales r_0 and r_1 have been related to properties of the charmonium spectrum which allows to determine them in physical units. We use here $r_0 = 0.469(7)$ fm as determined in Ref. [6]. More details on the scale setting procedure, as well as the parameterization of the LCP are given in Ref. [1].

3. The equation of state

Along the line of constant physics, at sufficiently large volume and at zero chemical potential, the temperature is the only intensive parameter that controls the thermodynamics. Consequently there exists only one independent bulk thermodynamic observable that needs to be calculated. All other quantities are then obtained by using standard thermodynamic relations. On the lattice, it is convenient to first calculate the trace anomaly in units of the fourth power of the temperature, $\Theta^{\mu\mu}/T^4$. It is easily obtained as a derivative of the pressure p/T^4 , with respect to the temperature,

$$\frac{\Theta^{\mu\mu}}{T^4} \equiv \frac{\epsilon - 3p}{T^4} = T \frac{\partial}{\partial T} (p/T^4). \quad (2)$$

As the pressure is directly given by the partition function, $p/T = V^{-1} \ln Z$, the calculation of the trace anomaly requires only the evaluation of rather simple expectation values. According to Eq. 2 one then obtains the pressure by

$$\frac{p(T)}{T^4} - \frac{p(T_0)}{T_0^4} = \int_{T_0}^T dT' \frac{1}{T'^5} \Theta^{\mu\mu}(T') . \quad (3)$$

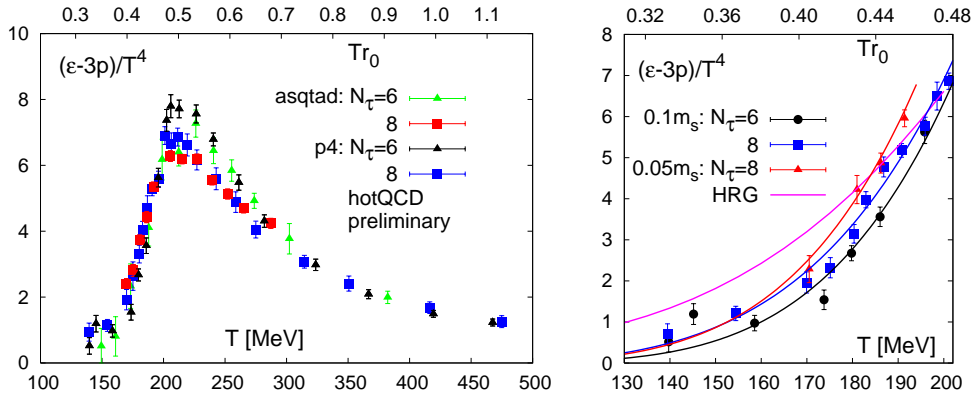


Fig. 1. The trace anomaly, $(\epsilon - 3p)/T^4$ on $N_\tau = 6$ and 8 lattices. On the left panel results are obtained with the p4fat3 and asqtad actions, where $N_\tau = 6$ results are from [1] and [7] respectively, $N_\tau = 8$ results are preliminary hotQCD results [2]. The right panel shows the low temperature part of the trace anomaly in detail, here we plot only results obtained by the p4fat3 action. Also shown on the right panel are quadratic fits to the data, as well as the trace anomaly obtained in the framework of the Resonance gas model. Light quark masses have been constrained to be one tenth of the strange quark mass ($0.1m_s$), on the right panel we show, however, also preliminary results from simulations with physical quark masses ($0.05m_s$) [4].

Here T_0 is an arbitrary temperature value which usually is chosen in the low temperature regime where the pressure and other thermodynamic quantities are suppressed exponentially by Boltzmann factors corresponding to the lightest hadronic states; e.g. the pions. The energy density is then obtained by combining results for p/T^4 and $(\epsilon - 3p)/T^4$, respectively.

In Fig. 1 (left) we show results for $\Theta^{\mu\mu}/T^4$ obtained with the asqtad and p4fat3 actions, respectively. The new $N_\tau = 8$ results [2] are compared to $N_\tau = 6$ results taken from [1,7]. We note that the asqtad and p4fat3 formulations give results which are in good agreement with each other. In fact, in quite a large temperature regime the agreement for given lattice extent N_τ seems to be better than one could expect in view of the overall cut-off dependence that is visible when comparing results for $N_\tau = 6$ and $N_\tau = 8$ more closely. They lead to a reduction of the peak height in $\Theta^{\mu\mu}/T^4$, which is located at $T \simeq 200$ MeV and to a shift of the rapidly rising part of $\Theta^{\mu\mu}/T^4$ in the transition region to smaller values of the temperature.

In Fig. 1 (right) we show quadratic fits to the data obtained by the p4fat3 action, to highlight the cut-off effects. It is evident, that the $N_\tau = 8$ data is shifted relative to the $N_\tau = 6$ data by about 8 MeV at low temperatures, $T \simeq 160$ MeV. This shift decreases to about 5 MeV at temperatures $T \simeq 190$ MeV.

Light quark masses have been constrained to be one tenth of the strange quark mass ($0.1m_s$), on the right panel we show, however, also preliminary results from simulations with light quark masses of $0.05m_s$. This again leads to a further shift in $\Theta^{\mu\mu}$ of approximately 5 MeV at $T \simeq 190$ MeV towards lower temperatures.

We also compare the results for $(\epsilon - 3p)/T^4$ to results obtained from the hadron resonance gas model. Details on the resonance gas curve in Fig. 1 (right) will be given in [2]. The slope of $(\epsilon - 3p)/T^4$ obtained by the resonance gas model seems to be much smaller than the slope obtained by the quadratic fits to the data. Whether this points

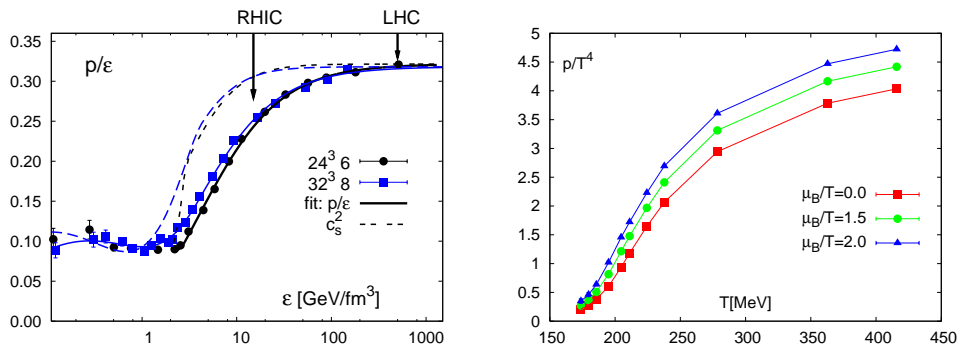


Fig. 2. The ratio of pressure and energy density as well as the velocity of sound obtained in calculations with the p4fat3 action on $N_\tau = 6$ [1] and $N_\tau = 8$ [2] lattices (left). The pressure in units of T^4 as function of temperature, for fixed and non-zero values of μ_B/T , obtained on $N_\tau = 6$ lattices (right).

at deviations of the equation of state at lower temperatures from resonance gas behavior or is due to larger cut-off effects in the low temperature regime requires further studies. We note that the lattice spacing becomes larger at lower temperatures and violations of flavor symmetry, which are inherent to the staggered fermion formulations at finite lattice spacing, thus will become more important.

The cut-off dependence observed in $\Theta^{\mu\mu}/T^4$ carries over to the calculation of pressure and energy density; the former is obtained by integrating over $\Theta^{\mu\mu}/T^5$ and the energy density is then obtained by combining results for p/T^4 and $(\epsilon - 3p)/T^4$. This is apparent in Fig. 2 (left) where we show the ratio p/ϵ obtained with the p4fat3 action on $N_\tau = 6$ [1] and $N_\tau = 8$ [2] lattices. Cut-off effects are still visible in the vicinity of the ‘softest point’ of the EoS, which is related to the peak position of $(\epsilon - 3p)/T^4$. We find that in the entire range of energy densities relevant for the expansion of dense matter created at RHIC, $\epsilon \lesssim 10 \text{ GeV/fm}^3$, the ratio p/ϵ deviates significantly from the conformal, ideal gas value $p/\epsilon = 1/3$.

This also is reflected in the behavior of the velocity of sound, $c_s^2 = dp/d\epsilon$, which is shown in Fig. 2 (left) by dashed lines. It starts deviating significantly from the ideal gas value below $\epsilon \simeq 10 \text{ GeV/fm}^3$ and reaches a value of about 0.1 in the transition region at energy densities $\epsilon \simeq 1 \text{ GeV/fm}^3$. Below the transition it slightly rises again, but note, that for very small temperatures c_s^2 , as well as p/ϵ are sensitive the integration constant $p_0(T_0)$ (see Eq. 2). At present we have set $p_0(T_0) = 0$, for $T_0 = 100 \text{ MeV}$.

4. Non-zero chemical potential

At non-zero chemical potential, lattice QCD is harmed by the “sign-problem”, which makes direct lattice calculations with standard Monte Carlo techniques at non-zero density practically impossible. However, for small values of the chemical potential, some methods have been successfully used to extract information on the dependence of thermodynamic quantities on the chemical potential. For an overview see, e.g. [8].

We closely follow here the approach and notation used in Ref. [9]. We start with a Taylor expansion for the pressure in terms of the quark chemical potentials $\mu_{u,d,s}$, we obtain

$$\frac{p}{T^4} = \sum_{i,j,k} c_{i,j,k}^{u,d,s}(T) \left(\frac{\mu_u}{T}\right)^i \left(\frac{\mu_d}{T}\right)^j \left(\frac{\mu_s}{T}\right)^k. \quad (4)$$

The expansion coefficients $c_{i,j,k}^{u,d,s}(T)$ are computed on the lattice at zero chemical potential, using stochastic estimators. Some details are given in [10,11]. We currently calculate the coefficients up to the 8th and 4th order, on $N_\tau = 4$ and 6 lattices, respectively. We find that cut-off effects are small and of similar magnitude as those found for the trace anomaly $\Theta^{\mu\mu}$ [11]. This was already anticipated by the analysis of the cut-off corrections in the free gas limit. Similar results for the asqtad action have been obtained in [12].

Alternatively to the quark chemical potentials one can introduce chemical potentials for the conserved quantities baryon number B , electric charge Q and strangeness S ($\mu_{B,Q,S}$), which are related to $\mu_{u,d,s}$ via

$$\mu_u = \frac{1}{3}\mu_B + \frac{2}{3}\mu_Q, \quad \mu_d = \frac{1}{3}\mu_B - \frac{1}{3}\mu_Q, \quad \mu_s = \frac{1}{3}\mu_B - \frac{1}{3}\mu_Q - \mu_S. \quad (5)$$

By means of these relations the coefficients $c_{i,j,k}^{B,Q,S}$ of the pressure expansion in terms of $\mu_{B,Q,S}$ are easily obtained, in analogy to Eq. 4

$$\frac{p}{T^4} = \sum_{i,j,k} c_{i,j,k}^{B,Q,S}(T) \left(\frac{\mu_B}{T}\right)^i \left(\frac{\mu_Q}{T}\right)^j \left(\frac{\mu_S}{T}\right)^k. \quad (6)$$

In Fig. 2 (right) we show the pressure expansion up to the fourth order in μ_B/T . The results are obtained on $N_\tau = 6$ lattices. We find that corrections to the pressure arising from a non-zero chemical potential are dominated by the second order expansion coefficient for moderate chemical potentials of $\mu_B/T \lesssim 2$ and are of the order of 10-20% for $T > T_c$.

5. Hadronic Fluctuations

Quark number fluctuations are obtained from derivatives of the QCD partition function with respect to the quark chemical potentials by the fluctuation-dissipation theorem. The Taylor expansion coefficients $c_{i,j,k}^{u,d,s}$, as defined in Eq. 4, can thus be directly interpreted as quark number fluctuations at $\mu = 0$. However, quark fluctuations can not be detected directly in experiments due to confinement. Therefore we will consider fluctuations in terms of hadronic quantum numbers, i.e. baryon number B , electric charge Q and strangeness S , which are more easily obtained by experiment. These fluctuations are related to the Taylor expansion coefficients $c_{i,j,k}^{B,Q,S}$, as given in Eq. 6. A recent overview on the physics of fluctuations in the context of heavy ion collisions was given in Ref. [13]. In general, the quadratic fluctuations χ_2^X at zero chemical potentials can be obtained from the second order coefficient c_2^X

$$c_2^X \equiv \frac{1}{2VT^3} \left. \frac{\partial^2 \ln Z}{\partial(\mu_X/T)^2} \right|_{\mu_{B,Q,S}=0} = \frac{1}{2VT^3} \langle (\delta N_X)^2 \rangle_0, \quad (7)$$

where $\delta N \equiv N - \langle N \rangle$ denotes the normalized net-density. and $\langle \dots \rangle_0$ indicates that the expectation value has been taken at $\mu_{B,Q,S} = 0$. Under such conditions, baryon number,

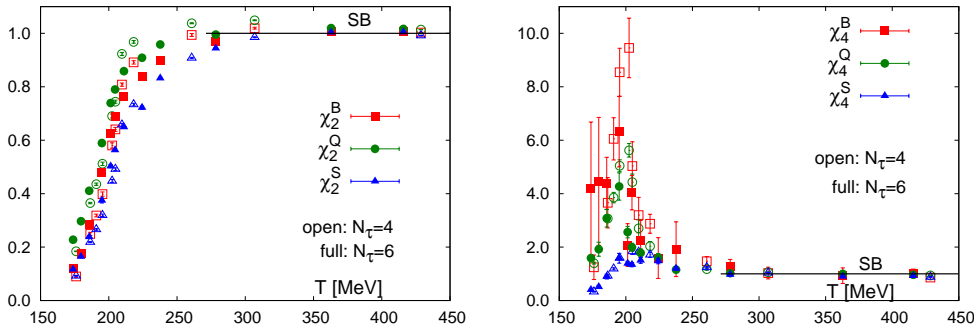


Fig. 3. Quadratic and quartic fluctuations of baryon number, electric charge and strangeness, normalized by their corresponding Stefan-Boltzmann value. The results on $N_\tau = 4$ lattices (open symbols) and $N_\tau = 6$ lattices (full symbols) are in good agreements.

electric charge and strangeness vanish, and we have $\delta N = N$. We define quadratic and quartic charge fluctuations by

$$\chi_2^X = \frac{1}{VT^3} \langle N_X^2 \rangle_0 = 2c_2^X, \quad \chi_4^X = \frac{1}{VT^3} (\langle N_X^4 \rangle_0 - 3\langle N_X^2 \rangle_0^2) = 24c_4^X, \quad (8)$$

respectively, and correlations among two conserved charges by

$$\chi_{11}^{XY} = \frac{1}{VT^3} (\langle N_X N_Y \rangle_0 - \langle N_X \rangle_0 \langle N_Y \rangle_0) = c_{11}^{XY}, \quad (9)$$

where $X, Y \in \{B, Q, S\}$.

In Fig. 3 we show results for quadratic and quartic fluctuations of B , Q and S . The quadratic fluctuations $\chi_2^{B,Q,S}$ rise rapidly in the transition region where the quartic fluctuations $\chi_4^{B,Q,S}$ show a peak. The peak height is more pronounced for the baryon number fluctuations than for fluctuations of the strange quarks.

We compare the results obtained on lattices with temporal extent $N_\tau = 4$ and 6. We notice that they are in general compatible with each other, especially in the high temperature phase, where both quadratic and quartic fluctuations approach the Stefan-Boltzmann limit quickly. The transition temperature has been previously determined to be $T_c = 202$ MeV and 196 MeV on $N_\tau = 4$ and 6 lattices respectively [14]. We thus conclude that at temperatures of about $1.5T_c$ and higher, quadratic and quartic fluctuations of B , Q and S are well described by the ideal massless quark gas.

At low temperature, hadrons are the relevant degrees of freedom. The hadron resonance gas (HRG) model has been shown to provide a good description of thermal conditions at freeze-out. We thus compare the fluctuations in the low temperature phase with a HRG model, where we include all mesons and baryons with masses smaller than 2.5 GeV from the particle data book.

In Fig. 4, we show the ratio of quartic and quadratic fluctuations for B , S and Q . In the HRG model, χ_4^B/χ_2^B is easily obtained in the Boltzmann approximation, which is valid for a dilute baryonic gas in the temperature range of interest. One finds that all details on the hadron mass spectrum and temperature dependence cancel and the result is a constant, given by the unit square of the baryonic charge (one for all baryons). This is in fact reproduced by the lattice results shown in Fig. 4 (top left).

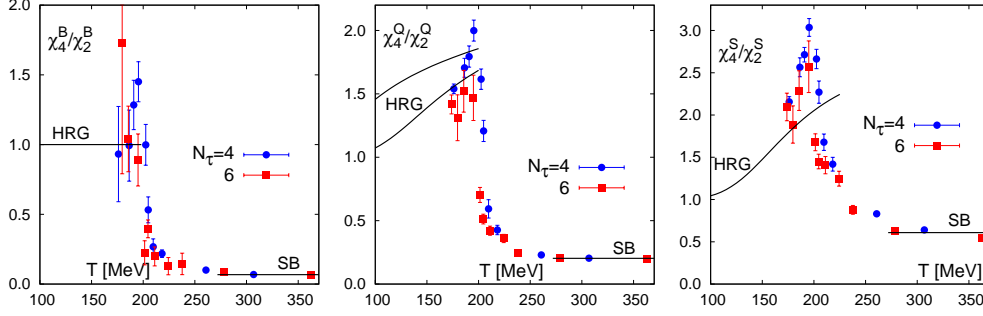


Fig. 4. Ratio of quartic and quadratic fluctuations of baryon number (B), strangeness (S) and electric charge (Q). The two curves of the HRG model in the top right figure correspond to charge fluctuations with physical pions (upper) and infinitely heavy pions (lower curve).

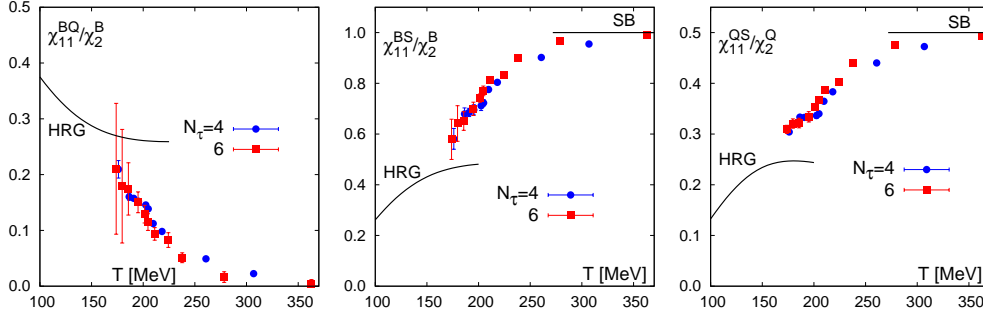


Fig. 5. Pairwise correlations of the conserved charges baryon number (B), electric charge (Q) and strangeness (S) as function of the temperature, normalized to the quadratic fluctuations of B and Q respectively.

The ratio of quartic and quadratic fluctuations for S and Q are more complicated even in the Boltzmann limit, since hadrons with different electric/strange charge give rise to different contributions to the corresponding fluctuations. For strangeness fluctuations, shown in Fig. 4 (bottom), the Boltzmann limit is still a good approximation; but for electric charge fluctuations, the pion mass plays an important role. In order to check for the sensitivity of electric charge fluctuations on the pion mass, we show in Fig. 4 (top right) results of a HRG model calculation with physical pion masses and without the pion sector, i.e. for infinitely heavy pions.

In Fig. 5, we show the various correlations χ_{11}^{BQ} , χ_{11}^{BS} and χ_{11}^{QS} normalized to quadratic fluctuations χ_2^B and χ_2^Q respectively. The results from $N_\tau = 4$ and 6 lattices agree with each other very well, and they are compared with the HRG model in the low temperature phase and Stefan-Boltzmann limit in the high temperature phase. We find that the correlations reproduce the qualitative behaviour of the HRG model below T_c and again start to agree with the free gas predictions for $T \gtrsim 1.5T_c$. The rapid suppression of fluctuations above T_c as well as the agreement of the correlations with the free gas predictions in the high temperature phase, suggests that in the quark-gluon-plasma the baryon number and electric charge are predominantly carried by quasi-particles, with the quantum numbers of quarks [15].

6. Conclusions

We have presented results on the equation of state on lattices of $N_\tau = 4, 6$ [1,7] and 8 [2] obtained with two different kinds of improved staggered fermions. Hadron masses have been kept constant in physical units and are chosen such that we have a physical strange quark mass (m_s) and 2 light quarks with a mass of $m_l = 0.1m_s$. We also presented some preliminary results with smaller quark masses $m_l = 0.05m_s$. We find that our two actions lead to a consistent picture of the thermodynamics of QCD and find in particular for the $N_\tau = 8$ results only small cut-off effects. We have calculated the equation of state as well as the velocity of sound and find the softest point of the equation of state to be $(p/\epsilon)_{min} \simeq 0.09$ at energy densities of $1 - 2 \text{ GeV}/\text{fm}^3$.

Furthermore, we calculated corrections to the equation of state arising from a non-zero baryon chemical potential, by means of a Taylor expansion of the pressure. Using the expansion coefficients, we have analyzed the quadratic and quartic fluctuations of baryon number, electric charge and strangeness, as well their ratios. We find these quantities to be in good agreement with the free gas results at temperatures of $T > 1.5T_c$. Below T_c , qualitative features of the resonance gas are reproduced. The ratio for the baryon number is closely related to the second approximation of the convergence radius of the Taylor series of the pressure with respect to the baryon chemical potential.

7. Acknowledgments

This work has been supported in part by contracts DE - AC02 - 98CH10886 and DE - FG02 - 92ER40699 with the U.S. Department of Energy. Numerical simulations have been performed on the BlueGene/L computers at Lawrence Livermore National Laboratory (LLNL) and the New York Center for Computational Sciences (NYCCS) as well as on the QCDOC computer of the RIKEN-BNL research center, the DOE funded QCDOC at Brookhaven National Laboratory (BNL) and the apeNEXT at Bielefeld University.

References

- [1] M. Cheng *et al.*, Phys. Rev. D **77** (2008) 014511.
- [2] HotQCD Collaboration, in preparation; F. Karsch, J. Phys. G **35** (2008) 104096; R. Gupta, PoS (**LAT2008**) (2008) 170, arXiv:0810.1764 [hep-lat].
- [3] I. Hováth, A. D. Kennedy and S. Sint, Nucl Phys. B **73** (1999) 834; M. A. Clark, A. D. Kennedy and Z. Sroczynski, Nucl. Phys. Proc. Suppl. **140** (2005) 835.
- [4] W. Söldner, PoS (**LAT2008**) (2008) 173, arXiv:0810.2468 [hep-lat].
- [5] C. Aubin *et al.*, Phys. Rev. D **70** (2004) 094505.
- [6] A. Gray *et al.*, Phys. Rev. D **72** (2005) 094507.
- [7] C. Bernard *et al.*, Phys. Rev. D **75** (2007) 094505.
- [8] M.P. Lombardo, J. Phys. G **35** (2008) 104019; C. Schmidt, PoS **LAT2006** (2006) 021.
- [9] C. R. Allton *et al.*, Phys. Rev D **71** (2005) 054508.
- [10] C. R. Allton *et al.*, Phys. Rev. D **66** (2002) 074507.
- [11] C. Miao and C. Schmidt, PoS **LAT2008** (2008) 172, arXiv:0810.0375 [hep-lat].
- [12] C. Bernard *et al.*, Phys. Rev. D **77** (2008) 014503.
- [13] V. Koch, arXiv:0810.2520.
- [14] M. Cheng *et al.*, Phys. Rev. D **74** (2006) 054507.
- [15] S. Ejiri, F. Karsch and K. Redlich, Phys. Lett. B **633** (2006) 275.